

## کانی‌های سولفوسالت بیسموت و پاراژنز آن‌ها در کانسار Cu-Ag-Au غنی از اسپیکولاریت قلعه‌زری (ایران)

کریم‌پور م.ح.<sup>۱</sup>، لارج ر.ر.<sup>۲</sup>، رزم‌آرا م.<sup>۱</sup>، پاتریک ر.ا.د.<sup>۳</sup>

۱- گروه زمین‌شناسی دانشگاه فردوسی مشهد

۲- مرکز تحقیقات ذخایر معدنی، دانشگاه تاسمانیا، استرلیا

۳- گروه علوم زمین، دانشگاه منچستر، منچستر، انگلستان

پست الکترونیکی: [mhkarimpour@yahoo.com](mailto:mhkarimpour@yahoo.com)

(دریافت مقاله ۸۴/۳/۲۶ ، دریافت نسخه نهایی ۸۴/۵/۲۶)

**چکیده:** کانسار Cu-Ag-Au غنی از اسپیکولاریت قلعه زری در ۱۸۰ کیلومتری جنوب شهرستان بیرجند و شرق ایران واقع شده است. سنگ‌های میزبان بیشتر از نوع آتشفشانی کالک‌آکالن غنی از پتاسیم و با سن  $2 \pm 40$  میلیون بوده و همچنین ماسه سنگ و شیل‌های ژوراسیک نیز یافت می‌شوند. سه رگه اصلی موازی و با شیب نزدیک قائم که سنگ‌های مختلف را قطع نموده‌اند در منطقه رخنمون دارند. کانسار قلعه زری از نوع Cu-Ag-Au غنی از اسپیکولاریت رگه‌ای است. چندین کانی سولفوسالت از سری‌های Ag-Cu-Pb-Bi و Pb-Bi در رگه‌های مختلف شناسایی شدند. بر اساس مطالعات پاراژنز و میکروترمومتری چهار مرحله مهم کانی‌سازی در منطقه شناسایی شدند. در مرحله اول اسپیکولاریت، کلریت، کوارتز، کالکوپیریت و سولفوسالت‌های بیسموت (ایکنیت، متالدیت و وتیچنیت) تشکیل شدند. دمای همگن شدن این مرحله  $380^\circ\text{C}$  تا  $290^\circ\text{C}$  است. در مرحله دوم پیریت، کالکوپیریت، کلریت، کوارتز، ایکنیت، کوسالیت، وتیچنیت، و کانی‌های سری بیسوتینیت-ایکنیت تشکیل شده‌اند. دمای همگن شدن این مرحله  $290^\circ\text{C}$  تا  $230^\circ\text{C}$  است. در مرحله سوم و چهارم اسپیکولاریت، کوارتز، کلسیت، پیریت، ایکنیت حاوی نقره و تعدادی کانی سولفوسالت غنی از نقره جدید شناسایی شدند. دمای همگن شدن این مرحله  $250^\circ\text{C}$  تا  $180^\circ\text{C}$  است. سولفوسالت‌های غنی از نقره حاوی بیشترین میزان Te, As, Sb, Se هستند. میزان املاح سیالات درگیر بین ۱ تا ۶ درصد NaCl و میزان  $\text{CO}_2$  کمتر از ۰/۱ مول بوده است. براساس پاراژنز کانی‌شناسی محلول گرمایی فوق اکسیدان بوده و  $\log f\text{O}_2$  بین ۱۳- تا ۲۸- بوده است. (در دمای  $300^\circ\text{C}$ ).

**واژه‌های کلیدی:** سولفوسالت، ایکنیت، متالدیت، وتیچنیت، معدن قلعه‌زری و ایران.



## **Bi- sulfosalt mineral series and their paragenetic associations in specularite-rich Cu-Ag-Au deposit, Qaleh-Zari mine, Iran**

**M. H. Karimpour<sup>1</sup>, R. R. Large<sup>2</sup>, M. Razmara<sup>1</sup>, R. A. D. Patrick<sup>3</sup>**

*1- Department of Geology, Ferdowsi University, Mashhad, Iran*

*2- Centre for Ore Deposit Research, University of Tasmania, Hobart, Tasmania, Australia*

*3- Department of Earth Sciences, University of Manchester, Manchester, M13 9PL, UK*

(Received: 16/06/2005, received in revised form: 19/08/2005)

**Abstract:** Qaleh-Zari specularite-rich Cu-Ag-Au deposit is located 180 Km south of Birjand, in eastern Iran. Host rocks are mainly Tertiary calc-alkaline to K-rich calc-alkaline of  $40.5 \pm 2$  Ma and Jurassic sandstones and shales. Three major sub-parallel steep quartz veins are identified in different rock types, in particular andesitic rocks. The Qaleh-Zari deposit is a specularite-rich hydrothermal, Cu-Ag-Au vein type deposit. Several complex Cu-Pb-Bi and Ag-Pb-Bi sulfosalt minerals have been identified in samples from different vein mineralization. Based on the paragenesis and fluid inclusion data temperature of homogenization, four ore-forming stages are identified in the area. In the first stage, specularite, chlorite, chalcopyrite and Bi-sulfosalts, (aikinite, matildite and wittichinite) were formed. The temperature of the homogenization of the fluid inclusions for the first stage ranges as 380 to 290°C. In the second stage, pyrite, chalcopyrite, chlorite, aikinite, cosalite, wittichinite and bismuthinite-aikinite were deposited. Homogenization temperature of fluid inclusions for the second stage of the mineralization are between 290 and 230°C. Within the third and fourth stages of the mineralization, specularite, quartz, calcite, pyrite, Ag-bearing aikinite, and an unknown Ag-sulfosalt were formed. The homogenization temperature for this stage ranges between 250 and 180°C. The unknown Ag-rich sulfosalts and arcubisite have the highest Te, As, Sb, and Se contents. The salinity of ore fluid was between 1.0 and 6.0 wt% equiv. NaCl and the CO<sub>2</sub> was < 0.1 mole%. Based on mineral paragenesis, the fluid was very oxidizing with a log  $f_{O_2}$  between -13 and -28 (assuming a temperature of 300°C).

**Keywords:** *sulfosalt, aikinite, matildite and wittichinite Qaleh-Zari mine, Iran.*

### Introduction

Sulfosalts are a subgroup of the sulfides that contain a diverse and complex group of minerals and synthetic compounds that have complex compositions and structures. Most of them are sources of economically important elements of ores (e.g. Cu, Ag, Cu, Bi, Hg and etc.) and some of them display semi-conducting properties, which have technological applications [1 to 5].

According to Makovicky [6] sulfosalts are defined as complex sulfides (rarely also selenides and tellurides) having the general formula  $A_mB_nX_p$  where:

A is a metal, commonly Cu, Pb, Ag and rarely Zn, Hg, Ti, Fe and Mn.

B is a typically a Group 15 semi-metal,  $As^{3+}$ ,  $Sb^{3+}$ ,  $Bi^{3+}$  but rarely also  $Te^{4+}$ .

X are anions usually  $S^{2-}$  but may also be partially substituted by  $Se^{2-}$  and  $Te^{2-}$ .

Sulfosalts appear in nature in major or trace amounts in a wide variety of ore deposit types, typically of hypogene hydrothermal origin but they are also formed by magmatic processes and occasionally occur in supergene conditions in zones of secondary enrichment. Sulfoantimonides and sulfoarsenides are abundant in low- and moderate-temperature deposits while sulfobismutides generally occur in higher temperature ores. Sulfoantimonides and sulfoarsenides have been discovered in modern hydrothermal formations on the ocean floor (the so-called black and white smokers, T about  $450^{\circ}C$  and  $230^{\circ}C$ , respectively) while sulfobismutides are recorded from active fumaroles (T =  $500 - 700^{\circ}C$ ) [5].

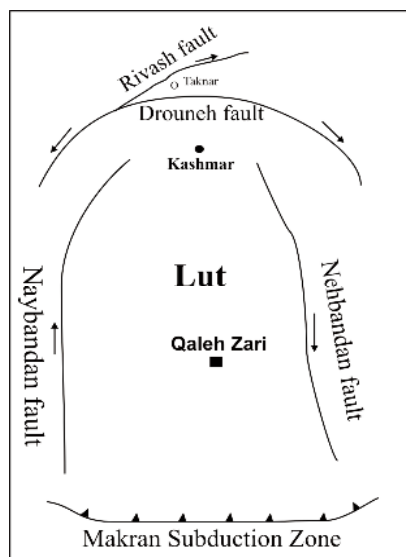
It should be stressed that even trace amounts of the sulfosalts in an ore are of both economic and scientific interest [5]. However, there is still a lack of reliable data on the characteristics of many of the sulfosalt minerals and synthetic phases, making them of interest for detailed studies of natural and synthetic systems.

### Geological setting

Qaleh-Zari is situated within the Central Lut Block at  $31^{\circ} 50' N$ ,  $59^{\circ} 00' E$  about 180 Km south of Birjand (Province of Khorasan) in the eastern part of Iran (Fig. 1). The Lut Block extends over 900 km in north-south direction and only 200 km wide in east-west direction. It is confined by Nayband fault and Shotori Range in the west and the Eastern Iranian Ranges in the east (Fig. 1). The western edge of the Lut Block is cut off by Nayband normal fault. A deformed accretionary prism and a flanking forearc basin extending from Birjand southeast to Zahedan (Fig. 1). Volcanic and some plutonic rocks of the Lut Block are the result of west dipping subduction zone.

The Lut Block is underlain by continental crust of some 40 km thickness [7]. The oldest sediments are from Devonian to Cretaceous time. Geological observation and radiometric data indicate the oldest magmatic activity in the Central Lut took place in the Jurassic time [8]. In Northern Lut Block, magmatic activity started in the Upper Cretaceous time (75 m.y.) both as volcanic and intrusive rocks.

**Fig. 1** Map showing the location of Qaleh Zari mine in central Lut region.



Maximum volcanic activity took place at the end of Eocene time. The Middle Eocene (47 m.y.) is distinguished by alkaline and shoshonitic volcanism [9]. In addition to calc-alkaline series, basalts and basaltic-andesite were formed in Eocene-Oligocene (40 to 31 m.y) and in Quaternary. The western part of the Central Lut Block is covered by terrestrial volcanic rocks [9]. In Shurab and Khur regions, Kerman Conglomerate occurs as a basis of volcanic sequence dated 39-40 Ma.

The oldest rocks exposed in Qaleh Zari area are Jurassic sandstones and shales which form the core of an anticline in the central part of the study area (Fig. 2). These are unconformably overlain by Upper Cretaceous conglomerates and sandy limestones (200 m). This sequence is followed by massive pale cream limestone (130 m) of Paleocene age. The Jurassic shales and sandstones in the Dom-e-Robah mountain area are unconformably (with an angular relationship of  $40^\circ$ ) by the reddish Upper Cretaceous conglomerates. Volcanic activity initiated in the region in the Late Eocene, and Tertiary volcanic rocks dominate the area. They consist of andesite, andesitic-basalts and minor dacite and basalts (Fig. 2) present as volcanic and pyroclastic rocks. Andesites from the western region of Qaleh-Zari were dated at  $40.5 \pm 2$  ma [10]. These rocks are calc-alkaline to K-rich calc-alkaline and have a geochemical signature typical of subduction-related magmatism [11, 12]. A highly altered intermediate intrusive rock (as a small exposure) is also reported from the area. The history of mining goes back more than 2000 years and at that time, mining reached only a shallow depth of 90 meters. Based on the observed old workings, the total ore mined in ancient times has been estimated to about 900 000 tons.

Three main mineralized zones were identified in the area. The NW part of the deposit (No. 1), which is associated with three major sub-parallel quartz

veins, the SE portion (No. 3) and the central part (the main vein set - No. 2). Volcanic rocks are host to the veins in No. 1 and No. 3 zones, whereas Jurassic shales and sandstones are the host rocks to the No. 2 zone. Four main trends of faults and joints (NW-SE, NE-SW and N-S sets) are identified in the area (Fig. 2). The NW-SE set is the oldest one and the main mineralization in the area is structurally confined to this set. The Qaleh-Zari mine is a specularite-rich Cu-Au-Ag vein-type deposit and limited previous studies have been carried out by Sadaghyani-Avval [11], Yuishi et al. [13], Daymeh Var [14] and Hassan Nejad [15].

#### **Analytical methods**

The samples were collected from the three main mineralized zones for petrography, fluid inclusion, XRD, electron microprobe, and isotopic studies. A series of polished blocks and thin sections were prepared for petrographic examination. X-ray diffraction was used to identify the major and minor minerals. For analysis of the sulfosalts, a CAMECA SX50 electron microprobe microanalyser with automated wavelength-dispersive and energy-dispersive analytical systems at the Central Science Laboratory (CSL), University of Tasmania was used. An accelerating voltage of 15 or 20 kV and a stable beam current of 20 or 30 nA were used. Some elements such as S and As were mobilized during analysis due to electron beam heating at 20 kV. In these cases a beam current of 15 nA was used during the electron probe microanalysis (EPMA). Six to nine points on grains of each mineral were analyzed. More than 60 grains of sulfosalts from different veins were subjected to EPMA. Sometimes grains were analyzed twice, depending on the size of the exposed surface to check for compositional zoning, twinning and exsolution, and to obtain a representative composition for the whole crystal. The detection limit was %Cu= 0.055, %Pb = 0.18, %Bi = 0.285, %Ag = 0.065, %S = 0.0, % Se = 0.025, Sb = 100 ppm, Te = 90 ppm, Au = 400 ppb, and Fe = 76 ppm. A Proton-Induced X-ray Emission (PIXE) study was carried out at the CSIRO Exploration and Mining, Sydney, Australia to analyze the trace element composition of the sulfide minerals.

A Fluid Inc. modified USGS heating/freezing stage was used for fluid inclusion study. The precision of the temperature measurements is better than  $\pm 1^\circ\text{C}$  for heating and  $\pm 0.3^\circ\text{C}$  for freezing. Accuracy of the measurements was insured by calibration against the triple point of  $\text{CO}_2$  ( $-56.6^\circ\text{C}$ ), the freezing point of water ( $0.0^\circ\text{C}$ ), the critical point of water ( $374.6^\circ\text{C}$ ) using synthetic fluid inclusions.

DILOR MICRოდIL-28® Raman microprobe at the Australian Geological Survey Organisation (AGSO), Canberra was used to quantitatively determine the composition of gaseous components (e.g.  $\text{H}_2\text{S}$ ,  $\text{CO}$ ,  $\text{CO}_2$ ,  $\text{CH}_4$ ,  $\text{SO}_2$ ,  $\text{H}_2$ ,  $\text{NH}_3$ ,  $\text{N}_2$ ) with a detection limit of 0.1 mole % for some species and to identify the daughter minerals in fluid inclusions from the deposit.

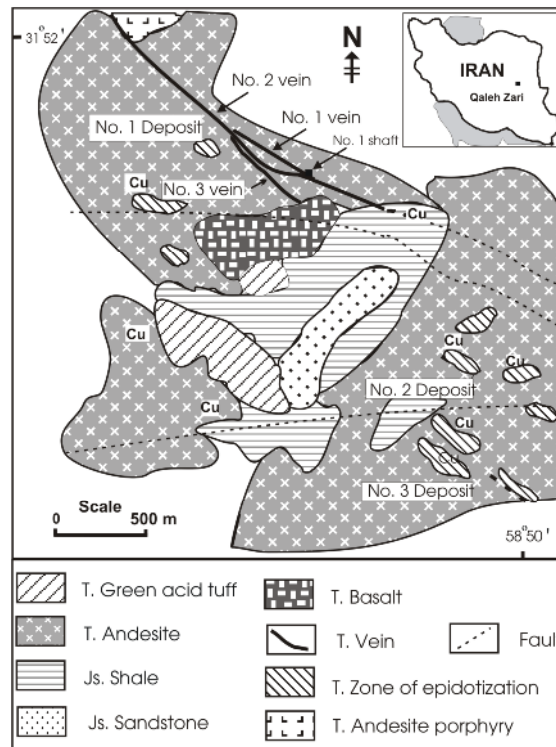


Fig. 2 Geological map of Qaleh-Zari area.

### Mineralization.

The mineralization in the area was controlled by a system of faults and joints. Four trends of faults and joints are identified in the mine area (Fig. 2). Three sets, 1)  $135/75^{\circ}\text{E}$ , 2)  $150^{\circ}/80^{\circ}\text{NE}$  and 3)  $30^{\circ}/70^{\circ}\text{SE}$  are right lateral strike-slip faults with reverse components, while the fourth set, 4)  $120^{\circ}/85^{\circ}\text{NE}$ , is a left-lateral strike slip fault with reverse components. The first stage of faulting was brittle and formed a wide zone of breccias, which were mineralized.

Quartz is the most common constituent in all of the veins, forming euhedral crystals, 1 to 10 cm long, and the quartz veins and veinlets typically have specularite bands at the margins (Fig. 3). Specularite makes up 10 to 25% of the veins and is the most abundant oxide after quartz. In all veins and veinlets, the general paragenetic sequence was: specularite followed by quartz–chlorite associations and finally chalcopyrite (Fig. 4). In one of the samples, electrum (Au, Ag) was identified (Fig. 5). Different sulfosalts characterize each stage of the mineralization.

Propylitic alteration assemblages are very widespread in the Qaleh-Zari area. Epidote and chlorite are the two characteristic minerals of this assemblage. Epidote is very abundant and formed by alteration of plagioclase, pyroxene, and hornblende. Epidote is also abundant as veinlets filling the joints.

Chlorite formed by alteration of mafic minerals or directly from the ore fluid within the vein (Fig. 3). Chlorites are generally Fe-rich types such as ripidolite with minor bronsvigite and pycnochlorite [16]. Argillic alteration is locally present. Silicification is mainly found within a zone adjacent to the veins.

The ore grade ranges between 2 to 9 wt% Cu, 100 to 650 ppm Ag and 0.5 to 35 ppm Au. On the basis of paragenesis and the temperatures of homogenization of fluid inclusions, the mineralization in the area can be divided into 4 stages.

**Fig. 3** Photomicrograph shows specularite (Sp) having bladed forms formed first then it followed by quartz and chlorite.



	Stage I	Stage II	Stage III, IV
<b>Temperature C</b>	380-290	290- 230	230-180
Specularite	●●●●●	●●●●●	●●●●●
Quartz	●●●●●	●●●●●	●●●●●
Chalcopyrite	●●●●●	●●●●●	●●●●●
Pyrite		■ ■ ■ ■ ■	
Aikinite (no inclusion)	.....		
Aikinite (Ag-rich or arcubisite inclusion)		- - - - -	
Aikinite (galena intergrowth)		- - - - -	
Galena (matildite exsolution)		.....	
Galena (Ag-rich inclusion)		.....	
Galena (wittichinite inclusion)		.....	
Galena (Aikinite intergrowth)		.....	
Wittichinite	.....		
Arcubisite		.....	
Matildite		.....	
Ag- rich sulfosalts		.....	
Bismuthinite- Aikinite series		■ ■ ■ ■ ■	
Cosalite & Berryite		.....	
Chlorite	-----		
Calcite			—————
Electrum	.....?		

**Fig. 4** Mineral paragenesis (hypogene) of Qaleh-Zari specularite- rich Cu-Au-Ag deposit



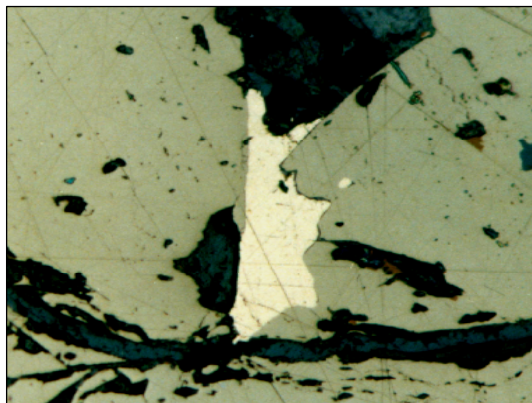


Fig. 5 Photomicrograph shows gold (electrum) grain within chalcopyrite.

**Stage I.** Comprises: specularite, quartz, chlorite, and chalcopyrite which is contemporaneous with the sulfosalts aikinite (without inclusions, Fig. 6), Matildite–galena, and wittichinite intergrowth with galena. Silver is present mainly in sulfosalt minerals such as matildite and wittichinite as well as sulfide (galena). Based on the fluid inclusion analysis, the temperature of the homogenization was determined as 380 to 290°C and the salinity was measured as between 5.0 and 3.0 wt % NaCl equivalent.

**Stage II.** Mineralogy: quartz, chalcopyrite, pyrite, chlorite, specularite, aikinite (with inclusions of Ag-rich sulfosalts, and intergrowths with galena), arcubisite, Ag-rich sulfosalts, galena (with Ag-rich inclusions), Ag-bearing aikinite, bismuthinite-aikinite solid solution series, berryite, Bi-bearing tetrahedrite and cosalite. The pyrite forms mainly euhedral crystals. The temperature of the homogenization, was determined as between 290 and 230°C and the salinity between 4.0 and 2.5 wt% NaCl equivalent.

**Stage III.** Mineralogy: quartz ± pyrite ± chalcopyrite ± Ag-rich sulfosalts ± arcubisite ± galena (with inclusions of Ag-rich sulfosalts).

**Stage IV.** Mineralogy: specularite, quartz, and ± calcite. Calcite is very abundant in the deposit of No 3.

The temperature of homogenization of fluid inclusions for the third and fourth stages of the mineralization was determined as between 250°C and 180°C. The salinity of fluid for this stage was between 2.3 to 1.3wt % NaCl equivalent. The CO<sub>2</sub> content was measured by Laser Raman spectroscopy and it is less than 0.1 mole %.

#### **Sulfosalt and their characteristic compositions**

In the Qaleh Zari area, aikinite (CuPbBiS<sub>3</sub>) is identified in all three types of the veins and it is anhedral and generally less than 0.2 mm in size (see Table 1 and Fig 6). Two generations of aikinite are recognized. In the first stage of mineralization, aikinite is homogeneous and found as inclusions in chalcopyrite. A second type of aikinite forms separate grains. Some grains

containing inclusions of Ag-rich sulfosalts and other grains intergrowths of aikinite and galena (Fig. 7). Some of the analyzed aikinite grains (e.g. sample L300-2, Table 1) contain excess Ag, which may occupy interstitial sites in the structure of aikinite.

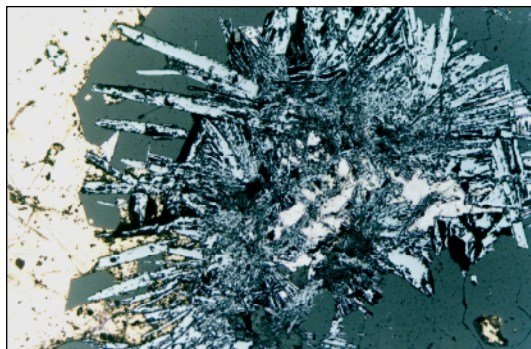


**Fig. 6** Photomicrograph shows that specularite and aikinite was formed first and (euhedral crystals of quartz and specularite) then it is followed by quartz and chalcopyrite.

**Table. 1** Representative microprobe data of aikinite and matildite.

Sample No.	Aikinite						Matildite		
	V-1, D-100, R30	V-1, D-100, L300	V-1, D-135, L250	V-1, D-170, L250	V-2, D-170, R250	V-3, Au-70	V-3, Au	V-1, D-100, R30	V-2, D-70, L100
<b>Pb</b>	34.84	34.5	34.87	35.16	34.27	34.66	n.d	n.d	n.d
<b>Ag</b>	n.d	n.d	0.4	n.d	n.d	n.d	28.6	28.48	28.13
<b>Bi</b>	36.46	35.26	35.66	35.53	36.77	37.2	52.33	52.47	54.57
<b>Cu</b>	11.05	10.53	10.04	10.44	10.23	10.32	0.07	0.16	0.075
<b>Fe</b>	0.1-0.5	n.d-0.8	n.d-0.08	0.01-0.04	0.02-0.03	n.d	n.a	n.a	n.a
<b>As</b>	n.a	n.a	n.a	n.a	n.a	n.a	n.a	n.d	n.d
<b>Sb</b>	n.d	n.d	n.d	n.d	0.02	n.d	n.a	0.06-0.15	0.03-0.04
<b>S</b>	16.66	16.65	14.66	16.27	16.35	16.56	15.88	15.24	16.43
<b>Se</b>	0.54	0.40	1.52	0.33	0.13	0.69	0.99	0.22	1.02
<b>Te</b>	0.07-0.21	n.d-0.16	0.02-0.12	0.02	0.01	0.16-0.25	n.a	n.d	n.d
<b>Total</b>	99.55	98.33	97.77	97.82	98.1	99.34	97.88	96.72	103
<b>Comments</b>	Inclusion in chalcopyrite				Isolated grain	Galena intergrowth	with galena		
<b>Empirical formula</b>	Cu <sub>0.99</sub> Pb <sub>0.96</sub> Bi <sub>0.99</sub> (S <sub>2.96</sub> Se <sub>0.04</sub> Te <sub>0.06</sub> ) <sub>3.06</sub>	Cu <sub>0.95</sub> Pb <sub>0.95</sub> Fe <sub>0.04</sub> Bi <sub>0.96</sub> (S <sub>2.97</sub> Se <sub>0.03</sub> ) <sub>3.00</sub>	Cu <sub>0.98</sub> Ag <sub>0.02</sub> Pb <sub>1.05</sub> Bi <sub>1.06</sub> (S <sub>2.85</sub> Se <sub>0.12</sub> Te <sub>0.03</sub> ) <sub>3.00</sub>	Cu <sub>0.96</sub> Pb <sub>0.99</sub> Bi <sub>1.00</sub> (S <sub>2.97</sub> Se <sub>0.02</sub> ) <sub>2.99</sub>	Cu <sub>0.94</sub> Pb <sub>0.97</sub> Bi <sub>1.03</sub> (S <sub>2.99</sub> Se <sub>0.01</sub> ) <sub>3.00</sub>	Cu <sub>0.93</sub> Pb <sub>0.95</sub> Bi <sub>1.01</sub> (S <sub>2.94</sub> Se <sub>0.05</sub> Te <sub>0.01</sub> ) <sub>3.00</sub>	Ag <sub>1.01</sub> Bi <sub>0.99</sub> (S <sub>1.95</sub> Se <sub>0.05</sub> ) <sub>2.00</sub>	Ag <sub>1.10</sub> Bi <sub>1.05</sub> (S <sub>1.99</sub> Se <sub>0.01</sub> ) <sub>2.00</sub>	Ag <sub>0.99</sub> Bi <sub>0.99</sub> (S <sub>1.95</sub> Se <sub>0.05</sub> ) <sub>2.00</sub>

n.d = not detected, n.a = not analyzed, V = Vein, D = Depth, Distance from shaft No.1 (L= left and R= right), the ideal composition of aikinite = CuPbBiS<sub>3</sub>, \* The ideal composition of matildite = AgBiS<sub>2</sub>.

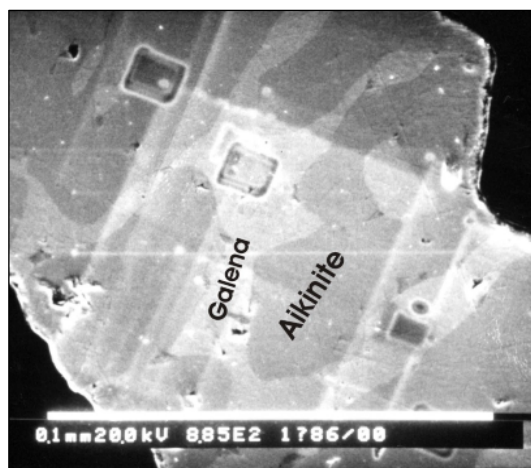


**Fig. 7** Back-scattered electron photograph of intergrowths or exsolution of aikinite and galena (sample 3-70, Au).

In the area, galena and matildite ( $\text{AgBiS}_2$ ) are found mainly together. In Fig. 8, matildite forms myrmekite-like intergrowths with galena. The similarities of crystal structure between the host phase galena (with space group,  $\text{Fm}\bar{3}\text{m}$ ) and the exsolved phase matildite (with the same space group) as well as matching atomic arrangements dictates that this exsolution is crystallographically controlled and also indicates a minimum precipitation temperature of 215 °C [17]. Arsenic and antimony are not detected in matildite (Table 1), consistent with low values of Sb/Bi in galena and a lack of miargyrite ( $\text{AgSbS}_2$ ), and absence of a solid solution series between matildite and miargyrite [18]. At Qaleh-Zari, two types of galena (typically 0.05-1 mm in size) are identified.

The first type is found mainly as small inclusions in chalcopyrite and most of these contain matildite (Table 2). This type of galena formed prior to the chalcopyrite in the first stage of the mineralization. The second type is formed as separate grains in the second stage of the mineralization. This type contains wittichinite or aikinite and they form myrmekite-like intergrowths (Fig. 7, 9).

The minor element contents of galena can point to genetic relationships and provide information about the condition of the formation of the ore deposit. Bismuth and antimony contents of galena have been used as indicators of conditions of ore deposit formation [19]. Malakhov [19] suggested that the ratio of Sb/Bi in galena provided qualitative information on the temperature and pressure, which existed at the time of their crystallization. Very low values ( $\text{Sb/Bi} < 0.6$ ) are characteristic of high temperature galena, which formed at pressures higher than  $250 \text{ kg/Cm}^3$ , while higher ratios ( $\text{Sb/Bi} > 6-13$ ) are typical of low-temperature galena which crystallized at relatively low pressure. In the area of the study a very wide fluctuation of Bi values in galena was noticed from different veins and

at different depths (1.2 to 6.92 wt %) but the Sb value is below the detection limit ( $Sb < 100$  ppm). Although ratios cannot be determined, a high temperature of formation of the galena is thus indicated. The Ag content of the galena is between 0.9 to 3.8wt% (Table 2). Several studies of natural galena [20, 21 & 22] suggest that the maximum low temperature minor element contents of galena are as followings: Bi, 5 wt%; Ag, 3 wt%; Sb, 3 wt%; Se 1.5 wt% and Cu 3000 ppm (Table 2). As can be seen the Ag and Bi contents are significant, perhaps enhanced by the coupled substitution of  $Ag^+ + Bi^{3+} \leftrightarrow 2Pb^{2+}$ ; certainly the latter might explain the very high values in L50. Coupled substitution might also be used to account for the high Cu values in the galena analyses, although alternatively sub-microscopic sulfosalts are also a possibility.

Wittichenite occurs mainly as small inclusions in chalcopyrite and very rarely in galena. It formed mainly in the first stage of mineralization. The wittichenite grains are homogeneous, do not contain any inclusions of other minerals and are anhedral with a grain diameter of less than 0.1 mm. Some wittichenite are found form myrmekite-like intergrowths with galena (Fig. 9). Wittichenite at the Qaleh-Zari contains silver in the range 1.5 to 7.86 wt% (Table 3, Fig. 10) which represents a solid solution in the range  $Cu_3BiS_3 - Ag_{0.5}Cu_{2.5}BiS_3$ .

**Fig. 8** Back-scattered electron photograph shows the exsolution or intergrowth texture matildite and galena.

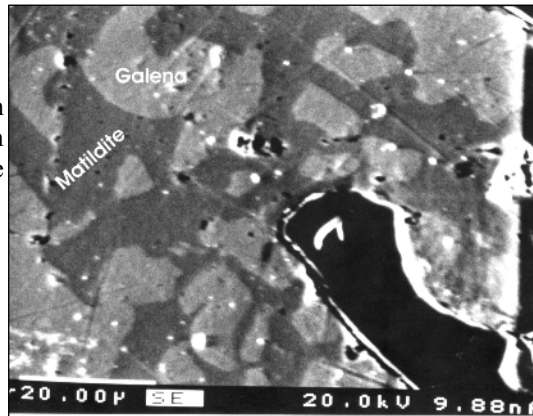


**Fig. 9** Photomicrograph shows that wittichenite and galena having myrmekite-like intergrowths texture.

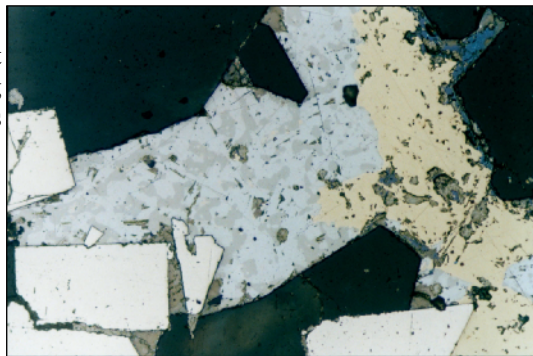


**Fig. 10** Plot shows the field of chemical composition of wittichinite and arcubisite from Qaleh-Zari and also some unknown Ag-rich sulfosalts.

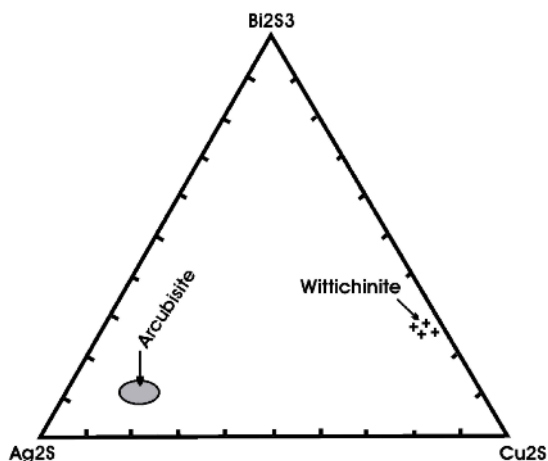


**Table 2** Microprobe data of galena from Qaleh Zari mine and other mine.

Sample No.	Galena						
	Qaleh Zari				Idarado mine (Colorado)	Jackass (California)	Pequea mine (Pennsylvania)
	V-3, D-70, L70	V-2, D-70 L50	V-3, D-70, Au2	V-3, D-70, Au1			
Pb	74.24	83.97	78.40	79.44	76-79.6	76	84.2
Ag	3.24	1.44	2.42	2.47	1.4-2.5	3.1	0.76
Bi	6.92	1.14	2.49	1.99	2.5-5.6	6.2	1.35
Cu	0.58	0.31	0.28	0.07	0.1-0.2	0	0.0015
Fe	n.a	n.a	n.a	n.a	n.a	n.a	n.a
As	n.a	n.a	n.a	n.a	n.a	n.a	<0.002
Sb	n.a	n.a	n.a	n.a	n.d	0.2	0.001
S	12.30	13.12	12.02	12.98	13.6-14.2	13.6	13.6
Se	1.15	0.39	2.49	1.20	n.a	n.a	0.028
Te	n.a	n.a	n.a	n.a	n.a	0	0.0012
Total	97.80	100.38	98.56	98.09	98-99	99.1	99.91
Comments	Isolated grains		With matildite	With aikinite	With Matildite	With Matildite	No inclusion
Empirical formula	(Pb <sub>0.96</sub> Ag <sub>0.08</sub> Cu <sub>0.02</sub> ) <sub>1.08</sub> (Sb <sub>0.96</sub> Se <sub>0.10</sub> ) <sub>1.00</sub>		(Pb <sub>0.97</sub> Ag <sub>0.03</sub> Cu <sub>0.01</sub> ) <sub>1.02</sub> (Sb <sub>0.99</sub> Se <sub>0.10</sub> ) <sub>1.00</sub>	(Pb <sub>0.93</sub> Ag <sub>0.05</sub> Cu <sub>0.01</sub> ) <sub>1.02</sub> (Sb <sub>0.92</sub> Se <sub>0.08</sub> ) <sub>1.00</sub>	(Pb <sub>0.91</sub> Ag <sub>0.05</sub> Bi <sub>0.02</sub> ) <sub>1.02</sub> (Sb <sub>0.96</sub> Se <sub>0.04</sub> ) <sub>1.00</sub>		

n.d = not detected, n.a = not analyzed, V = Vein, D = Depth, Distance from shaft No. 1 (L= left and R= right).

Arcubisite (Ag<sub>6</sub>BiCuS<sub>4</sub>) occurs as a myrmekitic intergrowth with aikinite but is not found as inclusions within chalcopyrite. Based on this textural relationship, they formed in the second stage of the mineralization and their average grain size is 0.09 mm. The major and minor element contents of arcubisite are reported in Table 3. The area where arcubisite plotted is shown

in Fig. 10. Although the formula of arcubisite of Qaleh-Zari is in the range of its ideal formula, but the amount of Se, Te and Sb are relatively higher.

The berrysite grains are anhedral, homogeneous, without inclusions, and with a grain diameter of less than 0.3 mm. One grain (sample 3-70-L70), has a formula of  $Pb_{1.93}(Cu_{1.53}Ag_{1.55})_{3.08}Bi_5(S_{10.29}Se_{0.13})_{10.52}$ , similar to that determined by Nuffield & Harris [23]. Another one (sample 1-135, R10) has the formula  $Pb_3(Cu_{3.05}Ag_{2.22})_{5.27}Bi_{6.94}(S_{15.6}Se_{0.19})_{15.79}$ , similar to that determined by Karup-Moller [24], indicating a range of stoichiometries for this phase. The mineral cosalite ( $Pb_2Bi_2S_5$ ) was also identified in one of the samples (sample 1-135, R10) (Table 4).

#### Trace element contents

Arcubisite has the highest Te content and which ranges between 500 ppm and 3.8 wt% (Fig. 11). The Te contents of each arcubisite grain changes drastically from point to point and the back-scattered electron (BSE) photomicrograph reveals that the Te distribution in sulfosalts is very irregular and does not follow any type of regular zoning.

The range of Se values in all the sulfosalts is 0.86 to 3.3 wt%, of the Sb content 100 ppm to 3.3 wt% and of the As content between not detected and 0.27 wt%. The arcubisite has the highest Se contents (0.1-3.21 wt %) (Fig. 12). As with Te, it appears that the Se content of the fluid increased in the later stages of the mineralization. Some of the arcubisite and unknown Ag-sulfosalts have the highest As and Sb contents (Fig. 13). The as content of arcubisite is between 80 and 2700 ppm and the as content of unknown Ag-sulfosalts is up to 3.24 wt% (Fig. 13), positive correlation exists between the As and Sb contents. It can be seen that there is no obvious correlation between Te and (As+Sb) contents of the sulfosalts of the area, although, usually, minerals with high value of Te have low (Sb+As) and those with high (As+Sb) carry low Te (Fig. 11). There is a relatively good positive correlation between Te and Se of the sulfosalts of the area (Fig. 12), but no correlation between their Se and (As+Sb) contents (Fig. 13).

**Fig. 11** Plot shows the Te and (As + Sb) content of some sulfosalts from Qaleh-Zari.

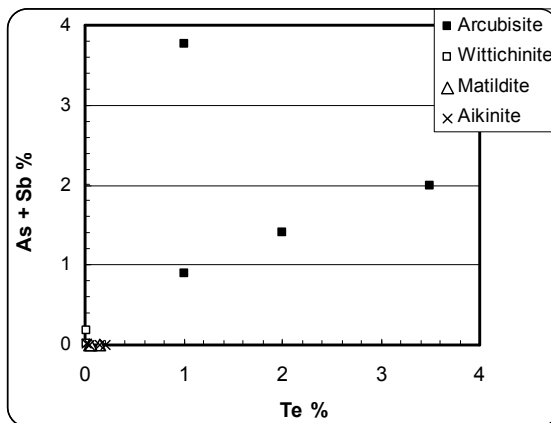


**Table 3.** Representative microprobe data of wittichinite and arcubisite

SampleNo.	Wittichinite				Arcubisite			
	1-100,L30	2-70,R250	2-170,R250	2-170, L250	2-70, L100	1-100, L30	2-170, R250	1-170, R10
Ag	7.86	6.08	4.24	1.51-3.47	57.98	58.27	58.5-59.4	63.3
Bi	40.3	40.24	40.5	40.4	12.06	12.6	15.6-17.1	9.37
Cu	33.2	33.14	33.76	35.18-36.18	10.50	9.98	6.9-7.5	9.6
Pb	n.d	n.d	n.d	n.d	n.d	n.d	n.d	n.d
S	17.2	17.04	17.9	18.3-18.82	13.51	13.06	10.93-11.17	14.99
Se	0.05	0.3-0.8	0.61	n.d-0.07	1.91	2.16	3.1-3.21	0.11
As	n.a	n.d-0.01	n.d	n.a	n.a	n.a	n.d	0.08-0.27
Sb	n.a	0.01	0.01	n.a	n.a	n.a	n.d-0.8	1.9-3.3
Te	n.a	0.02-0.11	0.18	n.a	n.a	n.a	0.9-3.77	1.4-1.9
Fe	n.a	0.3	0.13	n.a	n.a	n.a	0.05-0.92	0.6-0.92
Total	98.60	98.1	96.6	97.41	96.03	96.44	99.8-100.1	101.55
Comments	Isolated grain	In chalcopyrite	in chalcopyrite	in chalcopyrite	With aikinite			
Inclusion or zoning	no	no	no	no				
Empirical formula	(Ag <sub>0.41</sub> , Cu <sub>2.92</sub> )Bi <sub>1.08</sub> S <sub>3</sub>	(Ag <sub>0.31</sub> , Cu <sub>2.90</sub> )Bi <sub>1.07</sub> S <sub>3</sub>	(Ag <sub>0.21</sub> , Cu <sub>2.81</sub> )Bi <sub>1.02</sub> S <sub>3</sub>	(Ag <sub>0.12</sub> , Cu <sub>2.90</sub> )Bi <sub>1.00</sub> S <sub>3</sub>	(Ag <sub>6.03</sub> , Cu <sub>1.88</sub> )Bi <sub>0.65</sub> (S <sub>4.73</sub> , S <sub>5.00</sub> )	(Ag <sub>6.21</sub> , Cu <sub>1.81</sub> )Bi <sub>0.69</sub> (S <sub>4.68</sub> , S <sub>5.32</sub> )	(Ag <sub>6.78</sub> , Cu <sub>1.41</sub> )Bi <sub>0.97</sub> , Sb <sub>0.04</sub> Fe <sub>0.11</sub> (S <sub>4.28</sub> , S <sub>5.06</sub> , Te <sub>0.23</sub> )	(Ag <sub>6.08</sub> , Cu <sub>1.57</sub> )Bi <sub>0.46</sub> , Sb <sub>0.22</sub> Fe <sub>0.14</sub> (S <sub>4.85</sub> , S <sub>5.01</sub> , Te <sub>0.13</sub> )

n.d = not detected, n.a = not analyzed, V = Vein, D = Depth, Distance from shaft No.1 (L= left and R= right), The ideal composition of wittichinite = Cu<sub>3</sub>BiS<sub>3</sub>, The ideal composition of arcubisite = Ag<sub>6</sub>BiCuS<sub>4</sub>.

**Fig. 12** Plot shows Te versus Se content of some sulfosalts from Qaleh-Zari.

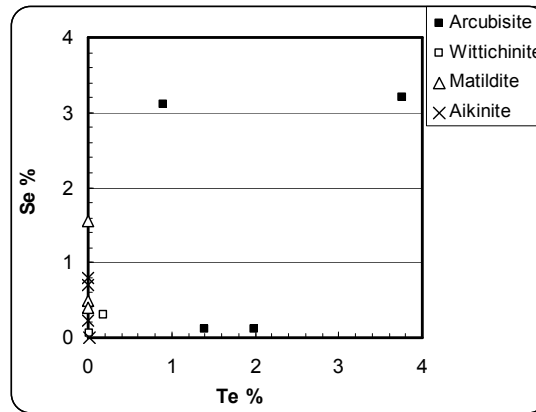


**Fig. 13** Se versus (As + Sb) content of some sulfosalts from Qaleh-Zari.

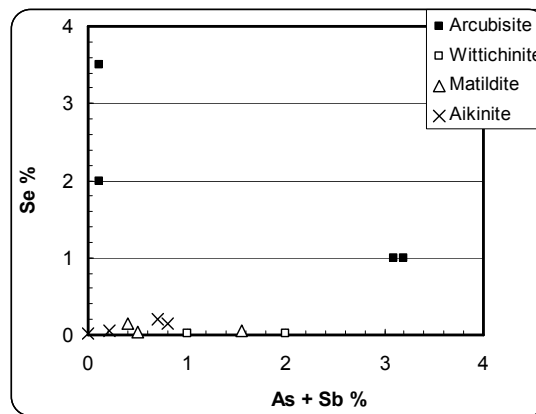


**Table 4.** Representative microprobe data of berryite and cosalite.

Element %	Berryite		Cosalite
	3-70, L70	1-135, R10	1-135, R10
Pb	18.89	20.33	38.40
Ag	7.9	7.8	3.64
Bi	49.94	47.16	41.26
Cu	4.6	6.27	0.185
Fe	n.a	n.a	n.a
Sb	n.d	n.d	n.a
S	15.56	16.27	14.99
Se	0.48	0.48	n.a
l-Total	97.7	98.33	98.48
Inclusion Zoning	No	No	No
Empirical formula	$Pb_{2.97}(Ag_{2.38}, Cu_{2.36})Bi_{7.78}(S_{15.80}, Se_{0.20})_{16.00}$	$Pb_{3.06}(Ag_{2.25}, Cu_{3.07})Bi_{7.03}(S_{15.80}, Se_{0.20})_{16.00}$	$Pb_{1.98}(Ag_{0.36}, Cu_{0.03})Bi_{2.11}, S_{5.00}$

The ideal composition of cosalite =  $Pb_2Bi_2S_5$ .

### Conclusions

Qaleh-Zari is a specularite-rich Cu-Ag-Au deposit and an oxidizing hydrothermal system. Based on paragenesis and temperature of homogenization of fluid inclusions, four stages of mineralization are identified in the area. More than 10 different types of sulfosalts are identified. At higher temperatures (385 to 295 °C), aikinite and wittichinite were deposited but at lower temperatures (250 to 180°C), arcubisite, cosalite, tetrahedrite and an unknown Ag-rich sulfosalt were formed. The salinity of fluid inclusions in the earlier stages was 5.8 wt % NaCl eq which decreased to 1.3 wt% in the final stages. The available data indicates that the chloride complexes were the probable main metal transport species early in the mineralizing episode but the later dilute solutions may indicate an increase in importance of bisulphide complexes.

### Acknowledgments

We would like to thank to Iranian industrial Copper company and Minakan Mining Company for their cooperation and assistance with respect to sampling and providing polished sections. In particular, we thank Mr. Abdi for helping to collect the samples. The authors wish to thank the director of Centre for Ore Deposit Research in University of Tasmania, Australia for his cooperation in accessing the research facilities. Thanks are also given to the staff of the Central Sciences Laboratory, University of Tasmania for helping with the EPMA. We highly appreciate the help of Dr Mozgova for his critical review of the earlier version of this manuscript. We are grateful to reviewers and referees of Iranian Journal of Crystallography and mineralogy, which helped to refine the article.

### References

- [1] Mozgova N. N., "Homologous series of sulfosalts (complex sulphides)", IX IMA meeting-74 (1974) Collected Abstracts, 116.
- [2] Mozgova N. N., "Regular micro intergrowths as a characteristic feature of homologous series of sulfosalts", 25<sup>th</sup> International Geological Congress, Abstracts (1977) 586-587



- [3] Mozgova N. N., "Principles of classification of sulfosalts", 27<sup>th</sup> International Geological Congress, Proceedings (1984) 53-65.
- [4] Mozgova N. N., "Non-stoichiometry and homologous series in sulfosalts. – Moscow", Nauka 264 (1985).
- [5] Mozgova N. N., "Sulfosalt mineralogy today: MODERN APPROACHES TO ORE AND ENVIRONMENTAL MINERALOGY" MSF Mini-Symposium, held in conjunction with IMA", Espoo Finland, June 11-17 (2000).
- [6] Makovicky E., "Modular classification of sulfosalts - current status", Neues Jahrbuch für Mineralogie, Abh., 160, 3 (1989) 269-297.
- [7] Dehghani G., "Schwerefeld und Krustenaufbau im Iran- Humburger Geophys", Einzelscher. R. A., H., 54, S. Hamburg. (1981)
- [8] Tarkian M., Lotfi M., Baumann A., "Magmatic copper and Lead Zinc ore deposits in the Central Lut, Eastern Iran", N. Jb. Geol. Palaont. Abh, 168, 2/3: 497-523 (1984).
- [9] Lensch G., Schmidt K., "Plate tectonic, orogeny, and mineralization in the Iranian fold belts results and conclusions", N. Jb. Geol. Palaont. Abh. 168, 2/3:558-568 (1984).
- [10] Kluyver H. M., Griffiths R. J., Tirrul R., Chance P.N., Meixner H. M., "Explanatory Text of the Lakar Kuh Quadrangle", Surv. of Iran (1978).
- [11] Sadaghyani-Avval F., "Etude geologique de la region de la mine de Khali-Eh-Zari (Iran) mineralization et inclusions fluids", PhD theses, Universite de Nancy I. 165. (1976)
- [12] Tarkian M., Lotfi M., Bauman A., Tectonic, "magmatism and the formation of mineral deposits in central Lut, East of Iran, Geol", Survey of Iran, Rep. No. 57 (1983) 357-383.
- [13] Yuishi S., Katsumi Ogawa, Niihito Akiyama, "Copper ores from Qaleh Zari mine", Iran. Mining Geology 26 (1976) 385-391.
- [14] Daymeh Var M., "Geology and geochemistry of Qaleh-Zari Cu-Au deposit", Unpublished MSc thesis, University of Tarbite Modares, Iran (1993).
- [15] Hassan Nejad A., "Geology and Geochemistry of Qaleh-Zari Cu-Au-Ag deposit", Unpublished MSc thesis, University of Shiraz, Iran. (1993)
- [16] Karimpour M. H., Khin Zaw, "Geochemistry and physicochemical condition of Qaleh-Zari Cu-Ag-Au ore bearing solution based on chlorite composition", Iranian J. of Crystallography and Mineralogy 8 (2000) 3-22.
- [17] Vaughan D. J., Craig J. R., "Ore microscopy and ore petrography", John Wiley (1994)
- [18] Razmara M. F., "The chemistry, structure and phase transitions of Ag(Sb, As, Bi)S<sub>2</sub> and Cu(Sb, Bi)S<sub>2</sub> solid solutions, and the effect of Cd, Hg and Zn substitutions into Ag(Sb, As, Bi)S<sub>2</sub> phases", PhD. thesis. University of Manchester 319 (1997)
- [19] Malakhov A. A., "Bismuth and antimony in galena, indicators of conditions of ore deposition", Geokhimiya 11 (1968) 1283-1296.
- [20] Flescher M., "Minor elements in some sulfide minerals", Econ. Geol. 50<sup>th</sup> Anniv., (1955) 970-1024.
- [21] Foord E. E., Shawe D. R., "The Pb-Bi-Ag-Cu-Hg chemistry of galena and some associated sulfosalts", A review and some new data from Colorado, California, and Pennsylvania. Can. Mineral. 16 (1989) 363-382.
- [22] Hall W. E., Heyl A. V., "Distribution of minor elements in ore and host rock, Illinois-Kentucky fluorite district and upper Mississippi Valley zinc lead district", Econ. Geol. 63 (1968) 655-670.
- [23] Nuffield E. W., Harris D. C., "Studies of minerals sulpho-salts: XX Berryite", a new mineral: Can. Mineralogist 8 (1966) 407-413.
- [24] Karup-Moller S., "Berryite from Greenland", Can. Mineral. 8 (1966) 414-423.